

# Development of a Multichannel Time-of-Flight Technique for Plasma Potential Profile Measurements by Heavy Ion Beam Diagnostic on the Tokamak ISTTOK

I.S. Nedzelskiy, A. Malaquias, Yu. I. Tashchev, C. Silva, H. Figueiredo, B. Gonçalves, H. Fernandes, C.A.F. Varandas

*Associação EURATOM/IST, Centro de Fusão Nuclear, Instituto Superior Técnico, 1049-001 Lisboa, Portugal*

**Abstract.** This contribution summarizes the current implementation of the time-of-flight (TOF) energy analysis for plasma potential measurements by the heavy ion beam diagnostic (HIBD) on the tokamak ISTTOK. The technique is described in detail. The results of the measurements of the ISTTOK plasma potential radial profile are presented. It is proved that the TOF energy analysis is suitable for simultaneous multichannel detection using a multiple cell array detector. With the aim of improving the signal-to-noise ratio of the diagnostic, the channeltrons have recently been installed on the “start” and “stop” detectors and preliminary results are discussed.

**Keywords:** Time-of-Flight, Heavy Ion Beam, ISTTOK

**PACS:** 50.52.55.-s, 52.55.Fa, 52.70.-m, 52.70.Nc

## INTRODUCTION

To obtain the measurements of the plasma potential by a heavy ion beam diagnostic (HIBD) with a multiple cell array detector (MCAD), an alternative multi-channel time-of-flight (TOF) energy analysis has been proposed [1,2] and developed on the tokamak ISTTOK [3-5].

This paper summarizes current implementation of the TOF technique on the ISTTOK HIBD. It includes short remind of the TOF method (Section II); description of the TOF technique (Section III); procedures of the measurements with the time-of-flight energy analyzer (TOFEA) (Section IV); first results of the plasma potential measurements (Section V); results of the preliminary tests of TOFEA operation with channeltrons (Section VI); conclusions and suggestions for further progress on the TOF method implementation (Section VII).

## TIME-OF-FLIGHT METHOD

Since the energy dispersion is created in time in the TOF method, a modulated incident beam must be used with a detection system capable of determining the time-

of-flight of the injected particles over a known distance (TOF-path). A detector at the entrance of the TOF-path creates the “start” (reference) signal, while the “stop” signal is obtained on the detector at the exit of the TOF-path. The TOF energy analysis is obtained by direct measurements of the “start”-“stop” time delay,  $t_{TOF}$ , of a single pulse modulated beam. The TOF HIBD measurements of the plasma potential,  $\Phi(l_{tr})$ , then are given by:

$$\Phi(l_{tr})/E_0 = -2[\Delta t_{TOF}/t_{TOF_{ss}}(\Phi=0)], \quad (E_0 \gg q\Phi_{max}), \quad (1)$$

where  $\Delta t_{TOF} = t_{TOF_{ss}}(\Phi \neq 0) - t_{TOF_{ss}}(\Phi = 0)$ ,  $t_{TOF_{ss}}$  is the time-of-flight between “start” and “stop” detectors arranged along secondary ion trajectories outside the plasma.

## TIME-OF-FLIGHT TECHNIQUE FOR PLASMA POTENTIAL MEASUREMENTS

ISTTOK HIBD [6] uses a  $Xe^+$  beam with 22 keV energy, 3 mm diameter, and up to 18  $\mu A$  of the beam current [7]. Beam modulation is obtained by a conventional electrostatic scanning of the beam across a slit. A four channel TOFEA has been developed and installed on ISTTOK, Fig. 1. A modified MCAD includes seven conventional cells and four TOFEA input slits. Because only the horizontal direction is available for the TOFEA arrangement, a turn-round of the secondary ions at  $30^\circ$  is necessary. It is achieved with a cylindrical electrostatic plate deflector (CEPD). The TOF-path module with “start” and “stop” detectors separated at a distance  $L_{TOF} = 620$  mm ( $t_{TOF_{ss}} = 3.475 \mu s$ ) follows the CEPD.

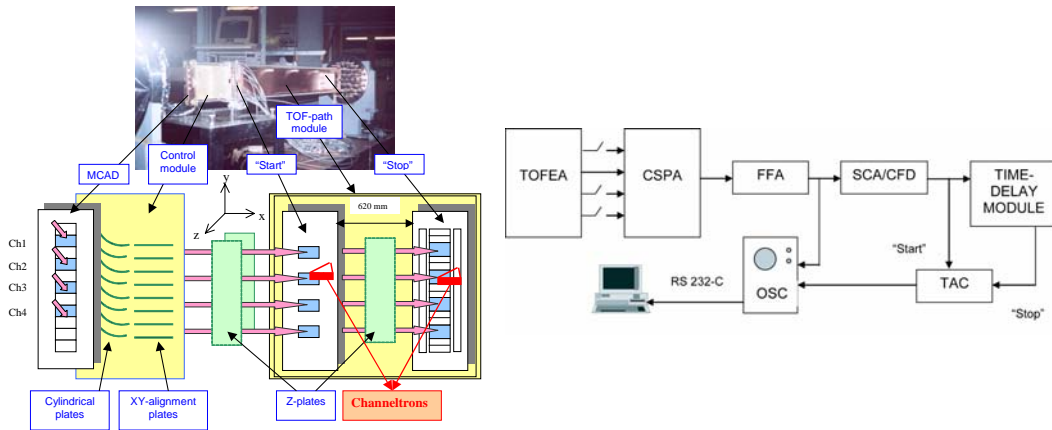


**FIGURE 1.** Picture and schematic of a four-channel TOFEA on ISTTOK with one channel DAS

The matrixes of “start” (a window of 80% transparency Ni mesh) and “stop” (copper plate) detectors are shown in Fig. 1 also. The additional above/below and left/right collectors control the beam alignment.

The data acquisition chain for one TOFEA channel includes a charge sensitive preamplifier (CSPA) (replaced by the current-to-voltage converter when working with

channeltrons), a fast-filter amplifier (FFA) and a single-channel analyzer/constant-fraction discriminator (SCA/CFD). The “start” and “stop” timing pulses are the inputs of the biased time-to-amplitude converter (TAC), which creates a pulse with an amplitude proportional to the time delay between them. The time-delay module (TDM) introduced between SCA/CFD and TAC allows fast and simple relative calibration of the TOFEA.

The adjustment of the DAS electronics to the experimental conditions is achieved by sending of a set of two successive test pulses (1.7  $\mu\text{s}$ , 3.475  $\mu\text{s}$  delay) with amplitude equivalent to the secondary beam signal from a pulse function generator. To preserve the real noise source, the CSPA input is simultaneously connected to the “start”-“stop” detectors. The width of the amplitude spectrum obtained by a multichannel analyzer (MCA) is then minimized by tuning the electronics parameters.

## PROCEDURES OF THE MEASUREMENTS WITH TOFEA

Experiments with the TOFEA have been performed in the tokamak ISTTOK ( $R = 0.45$  m,  $a_{\text{lim}} = 0.078$  m) discharges with  $I_p = 5$  kA,  $B = 0.45$  T,  $\langle n_e \rangle = (2.5-4.5) \times 10^{18} \text{ m}^{-3}$ ,  $T_e \sim 100$  eV.

Resolution of the TOFEA have been effectively investigated in the above optimization procedure without plasma. The dependence of the standard deviation of the TAC signal amplitude spectrum,  $w/2$ , on the signal-to-noise ratio (SNR) was measured by varying the test pulse amplitude. Fig. 2 shows an example of typically observed spectra. The obtained dependence of standard resolution of the measurements for different SNR is shown also. As an example, the value of the standard deviation  $w/2 \sim 35$  ns in Fig. 2 determines a standard resolution of  $\Delta\tau_{\text{TOF}}/\tau_{\text{TOF}} \sim \pm 1 \times 10^{-2}$  for a SNR  $\sim 9$ . Data presented in Fig.2 shows that it is possible to distinguish spectra with an 8 ns delay or with an order of magnitude better resolution.

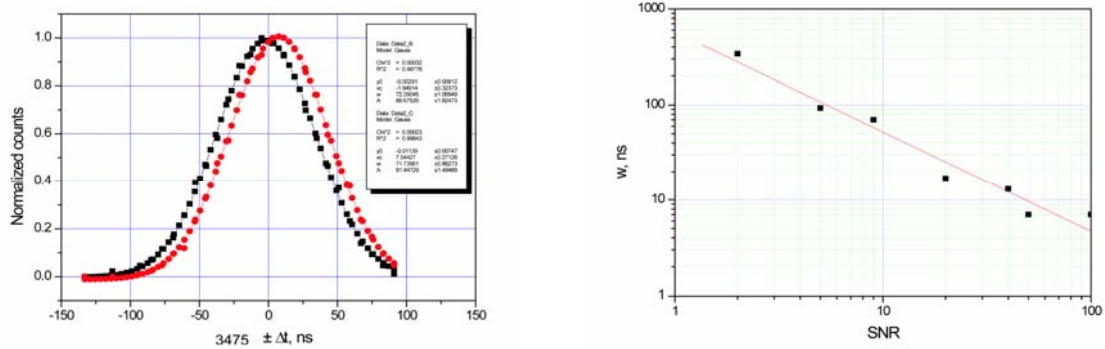


**FIGURE 2.** Spectrum of the TAC signals (two 1.7  $\mu\text{s}$  pulse) and its standard deviation spectrum with 8 ns delay, and dependence of the standard deviation on SNR.

The above results suggest the use of a statistical approach in the analysis of the plasma potential measurements by TOFEA. Resolution of the measurements can be estimated with the following statistic relation:

$$x_{es} = \langle x \rangle \pm (w/2) t_{N-1, \alpha} / (N)^{1/2}, \quad (2)$$

where  $x_{es}$  and  $\langle x \rangle$  are respectively the estimate and mean of the measured value,  $t_{n-1,\alpha}$  is the Student constant and  $N$  is the number of TAC output pulses. In the above example of  $SNR \sim 9$ , it gives  $\Delta\tau_{TOF}/\tau_{TOF} \sim \pm 2 \times 10^{-3}$  ( $\Delta\tau_{TOF} \sim \pm 7$  ns) with 90% confidence ( $t_{n-1,\alpha} \sim 1.66$ ) for 70 counts obtained during 1 ms time window of plasma shot with 15  $\mu$ s pulse repetition rate.

To determine the time-of-flight modified by the plasma potential, we use its calculated value for the beam pulse propagation along the TOF-path with initial energy, and an effective “start”-“start” TOFEA calibration. This calibration procedure is performed in the real measuring conditions and consists of registration on “start” detector of the real signals of the secondary ions created in plasma by two successive primary beam pulses with a duration of 1.7  $\mu$ s and calibrated delay of 3.475  $\mu$ s. Calculated mean level of the TAC signals presents a reference for the following measurements of TOF modification due to the plasma potential.

## RESULTS OF THE PLASMA POTENTIAL MEASUREMENTS

Fig. 3 exhibits an example of the TAC “start”-“start” calibration series, and the “start”-“stop” series obtained for Ch3 with indication of the respective mean levels. This data was obtained during the flat-top part of a plasma shot with a line-averaged electron density  $\langle n_e \rangle = 4.5 \times 10^{18} \text{ m}^{-3}$ . A value of  $\Phi_{pl}(\text{Ch3}) \sim -240 \pm 44 \text{ V}$  can be derived. The plasma potential measured in three points inside the plasma core and plasma periphery (probes) is shown in Fig.3. Notice the expected negative potential in the plasma core.

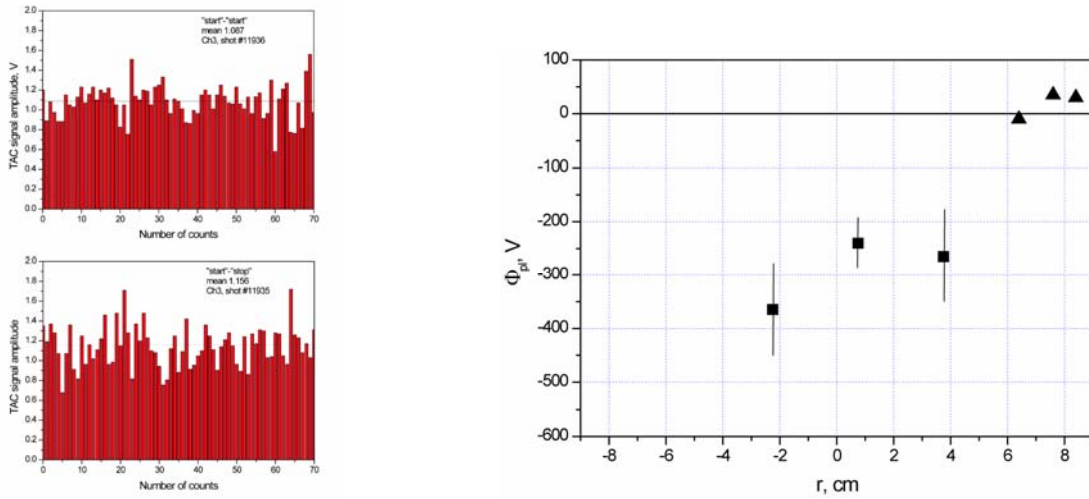


**FIGURE 3.** Histogram of the TAC signal in the “start”-“start” and “start”-“stop” series; and plasma potential measured by the TOFEA (cubes) and electric probes (triangles).

## PRELIMINARY TESTS OF TOFEA OPERATION WITH CHANNELTRONS.

To improve the measurements, the TOFEA energy resolution must be increased. It can be achieved with the use of electron multipliers (channeltron) as the “start”/“stop” detectors. The effective transparency for the “start” detection could be achieved by using of only a part of the channeltron horn to gather the secondary ions [5]. To check this idea, the channeltron has been first tested on primary Xe<sup>+</sup> beam inside the HIBD injector.

In these tests the beam is formed with 1 mm aperture, and the channeltron can be mechanically moved across the aperture. The obtained results are shown in Fig. 4, and confirm the reliability of the use of the channeltron in the TOFEA in the considered scheme.

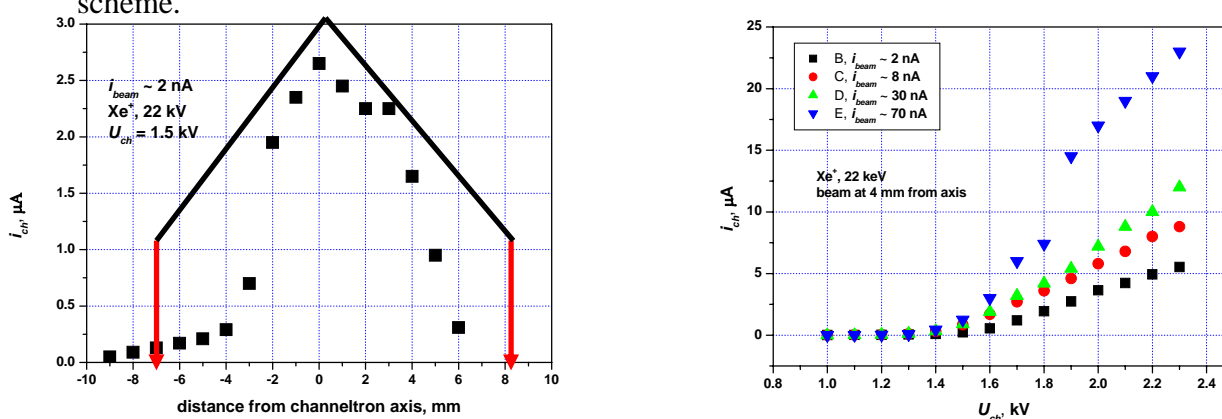


**FIGURE 4.** Distribution of the channeltron output current across channeltron horn, and its dependence on applied voltage with beam position at 3 mm from the edge of the channeltron horn.

Two similar channeltrons have been installed as the “start” and “stop” detectors in one channel of the TOFEA (Fig. 1). Fig. 5 presents signals obtained on the “start” grid and “start” and “stop channeltrons in a plasma shot obtained during secondary, Xe<sup>2+</sup>, beam alignment with a slow (1.5 ms) modulation of the primary beam.

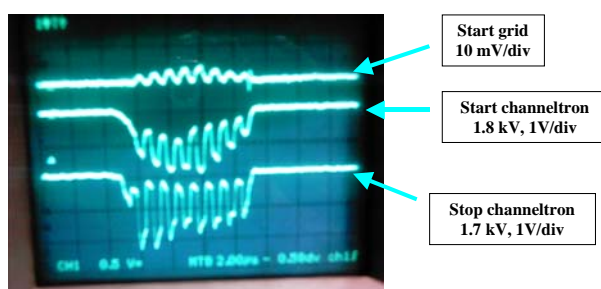


**FIGURE 5.** Signals from “start” grid and “start”-“stop” channeltrons (1.5 ms modulation).

The gain of  $\sim 102$  can be estimated. However, the observed signal clearly shows the presence of some initial level attributed to the sensitivity of the channeltrons to the

not completely shielded plasma radiation. After an additional more careful shielding has been introduced, an order of magnitude reduction of the parasitic signal has been achieved. Yet, when connected to the current-to-voltage converter, the noise generated by plasma still exists, keeping the same SNR as in experiments without channeltrons.

## CONCLUSIONS AND SUGGESTIONS FOR FUTURE WORK

The results of this work prove feasibility of the multichannel TOF energy analysis for the plasma potential profile measurements by the HIBD with MCAD. The first results of the plasma potential measurements have been obtained. However, the resolution of the measurements must be increased. Preliminary tests of channeltrons as “start”-“stop” detectors, though demonstrating their principal feasibility in the TOFEA operation, show a need for the careful shielding of the plasma radiation. These will be investigated in nearest tests in a scheme with additional ion/electron converters shown in Fig. 6.

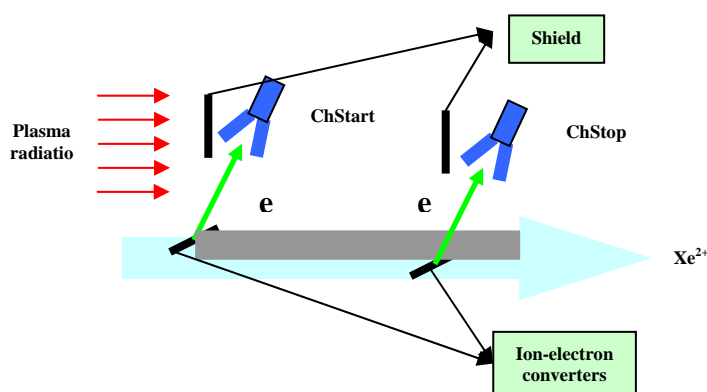


FIGURE 6. TOFEA with channeltron detectors and ion-electron converters.

## ACKNOWLEDGMENTS

This work has been carried out in the frame of the Contract of Association between the European Atomic Energy Community and Instituto Superior Técnico (IST) and of the Contract of Associated Laboratory between Fundação para a Ciência e Tecnologia (FCT) and IST. The content of the publication is the sole responsibility of the authors and it does not necessarily represent the views of the Commission of the European Union or FCT or their services.

## REFERENCES

1. I. S. Nedzelskiy, A. Malaquias, J. A. C. Cabral, C. A. F. Varandas, and V. Plyusnin, ICPP-2000 Conference, Quebec, Canada, 23-27 October 2000.

2. I. S. Nedzelskiy, A. Malaquias, J. A. C. Cabral, and C. A. F. Varandas, *Rev. Sci. Instrum.* **72**, 572 (2001).
3. I. S. Nedzelskiy, A. Malaquias, B. Gonçalves, C. A. F. Varandas, and J. A. C. Cabral, *Problems of Atomic Sci. and Technology* **5**, 148 (2002).
4. I. S. Nedzelskiy, A. Malaquias, B. Goncalves, C. Silva, J. A. C. Cabral, and C. A. F. Varandas, *Rev. Sci. Instrum.* **75**, 3514 (2004).5. B. R. Jackson and T. Pitman, U.S. Patent No. 6,345,224 (8 July 2004)
5. I.S. Nedzelskiy, A. Malaquias , Yu. Tashchev , C. Silva , H. Figueiredo , H. Fernandes , C.A.F. Varandas, *Review of Scientific Instruments*, **77**, 033505 (2006).
6. J. A. C. Cabral, O. J. Hancock, A. J. T. Holmes, M. Inman, C. M. O. Mahony, A. Malaquias, A. Praxedes, W. van Toledo, and C. A. F. Varandas, *Plasma Sources Sci. Technol.* **3**, 1 (1994).
7. J. A. C. Cabral, I. S. Nedzelskiy, A. J. Malaquias, B. Gonçalves, and C. A. F. Varandas, I.S. Bondarenko, S. M. Khrebtov, A. D. Comarov, A. L. Kozachek, and L. I. Krupnik, *Rev. Sci. Instrum.* **74**, 1853 (2003).